

Novel light coupling systems devised using a Harmony Search algorithm approach

I. Andonegui¹, Itziar Landa-Torres², Diana Manjarres² and A. J. Garcia-Adeva¹

¹ Department of Applied Physics I.
University of the Basque Country UPV/EHU, 01006 Vitoria, Spain

`imanol.andonegui@ehu.eus`

² TECNALIA, E-48160 Derio, Spain,
`itziar.landa@tecnalia.com`

Abstract We report a critical assessment of the use of an Inverse Design (ID) approach steamed by an improved Harmony Search (IHS) algorithm for enhancing light coupling to densely integrated photonic integrative circuits (PICs) using novel grating structures. Grating couplers, performing as a very attractive vertical coupling scheme for standard silicon nano waveguides are nowadays a custom component in almost every PIC. Nevertheless, their efficiency can be highly enhanced by using our ID methodology that can deal simultaneously with many physical and geometrical parameters. Moreover, this method paves the way for designing more sophisticated non-uniform gratings, which not only match the coupling efficiency of conventional periodic corrugated waveguides, but also allow to devise more complex components such as wavelength or polarization splitters, just to cite some.

1 Introduction

Electronics made possible to achieve a massive shrinking of the core electrical elements into chip scale building blocks. Likewise, silicon on insulator (SOI) technology has the capacity to overcome the integration scaling of electronics by enabling the mass production of large scale and dense integration of PICs. These high index contrast materials are an outstanding platform for designing compact devices consisting on low loss waveguides, splitters/combiners, wavelength multiplexers and i.e. a wide variety of integrated components. In the same line, the ongoing trend is to integrate these components on a single platform. However, the high integration density of such devices and i.e. their small feature size complicates the light coupling interfacing between standard single mode optical fibres (SMF) and SOI circuits, causing high insertion losses and high packaging costs. This decoupling is mainly due to the huge mode mismatch between the cross-sections of fibres and SOI guides [1]. To accomplish the fibre-chip coupling issue, two main strategies have been proposed so far: butt-coupling schemes and out-of-plane coupling solutions. Butt-coupling methods provide wide bandwidth and low insertion loss operation [2], but these kind of solutions require a lensed,

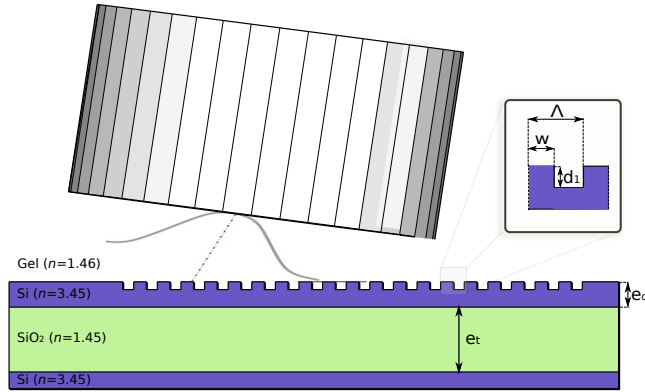


Figure 1. Basic configuration for a custom fiber-to-chip periodic grating coupler. A standard SMF interfaces near vertically with a diffractive grating structure defined on the surface of the silicon waveguide. The grating coupler structure is determined by the duty cycle (W), the filling factor (ff), the period (Λ) and the depth of the grooves (d_1). The rib waveguide consists of a silicon layer of thickness, etching depth (e_d) on top of a buried oxide layer (BOX) of thickness e_t . To clearly illustrate the design, the diagram is not to scale.

high numerical aperture fibre or an inverted taper with a very sensitive fiber-guide alignment [3, 4] to match the optical mode size between two light guiding materials. In contrast, out-of-plane coupling presents some major advantages over the former method: using this approach eludes the need of cleaved facet fibres and there is no limitation for extracting/coupling light everywhere on the chip, which is a critical advantage for large scale wafers [2]. Regular solutions provide guided-mode resonances using periodic gratings which have been widely demonstrated [5, 6]. Nevertheless, periodic grating designs present a small coupling strength, are rather long, working on not wide enough bandwidth.

The principle of periodic diffraction gratings for coupling light into a SMF is shown in Figure 1. Throughout this work we present a broad comparative study of non uniform grating structures for boosting the light coupling under different criteria beyond the limitations of standard periodic designs.

2 A deterministic search: finding the optimum

Figure 1 shows the schematic structure of a naive grating coupler defined on a regular SOI wafer with a 250 nm thick crystalline silicon layer which refractive index n is, $n = 3.467$, over a 2 μm thick buried oxide $n = 1.46$ layer. A single mode fibre is positioned with a tilt angle to the normal direction above the grating to avoid backreflection. In order to eliminate the fibers facet reflection, an index-matching gel $n = 1.46$ is utilized to fill the space between the fibre and the grating. Aside from the consideration of these parameter, it is of practical relevance to choose the etching depth and the period of the grating. Aside from

this toy-model case, when the amount of degrees of freedom involving the design process is large, it is impractical to determine the optimum, neither it is practical to do a thorough exploratory search among the whole set of feasible parameters. Thus, in order to show a simplified stage, wherein a brute-force hard search is still feasible, we delimited the search to the exploration of two coupled trivial parameters, i.e. to the duty cycle of the grating coupler W that defines the width of the grating tooth and the fill factor ff defined as the ratio of the grating period and the duty cycle ($ff = \Lambda/W$). Nonetheless, simplifying the designing parameters and assuming only a two parameter space search means that one should intuitively fix any other parameters. In this case we fixed the value of some parameters according to pure intuition and experimental lore, such as the position of the SMF fibre to $1.8 \mu\text{m}$ from the silicon top layer and to $5 \mu\text{m}$ in the horizontal axis from the grating edge, with a the tilt angle of 8° . The grating is devised by performing a 70 nm deep etching. Thus, we constrained the search to only these two parameters and we mapped the maximum coupling efficiency between a transverse electrically (TE) polarized Gaussian beam centred at $\lambda = 1.55\mu\text{m}$, where λ is the light's wavelength, spanning $0.1\mu\text{m}$, into a $10.4\mu\text{m}$ cross-section SMF. This configuration was modelled by means of two-dimensional Finite-Differential Time-Domain (FDTD) simulations with a uniform grid featuring elements with sizes bellow $\lambda/10$ and we used Perfectly Matched Layer (PML) boundary conditions surrounding the whole grating and fibre domains. The coupling efficiency (η) can be calculated by means of the following integral [7]:

$$\eta = \left| \int \int E_x E_{(y=y_0,z)} A e^{-\frac{(x-x_0)^2+(z-z_0)^2}{\omega_0^2}} e^{jn \frac{2\pi}{\lambda} z \sin \Theta} dx dz \right|, \quad (1)$$

where Θ is the fibre tilt angle, (x_0, y_0, z_0) is the position of the fibre with respect to the grating coupler, n is the refractive index on top of the grating and the constant A represents the normalization of the Gaussian beam.

Figure 2.a depicts the coupling proficiency of 10.000 combinations of ff and W computed in a regular *i3* computer where it took around 72 hours to complete it. As expected in this trivial case, an almost linear relation between the filling factor and the duty cycle can be appreciated along with some global maxima remarked in black. In addition, we assumed that the oxide thickness, fibres tilt angle, etching deep and some other aforementioned parameters were almost optimal for a minimal downward leakage, but that is not necessarily true since all these parameters are coupled to each other. Therefore, it is infeasible to do these kind of intensive calculations when the parameter space is increased using a deterministic search.

3 The IHS algorithm for non-deterministic search of optima

Except of the trivial case comprised by only 2 parameter data sets discussed in Section 2, when more parameters are taken into account, a deterministic

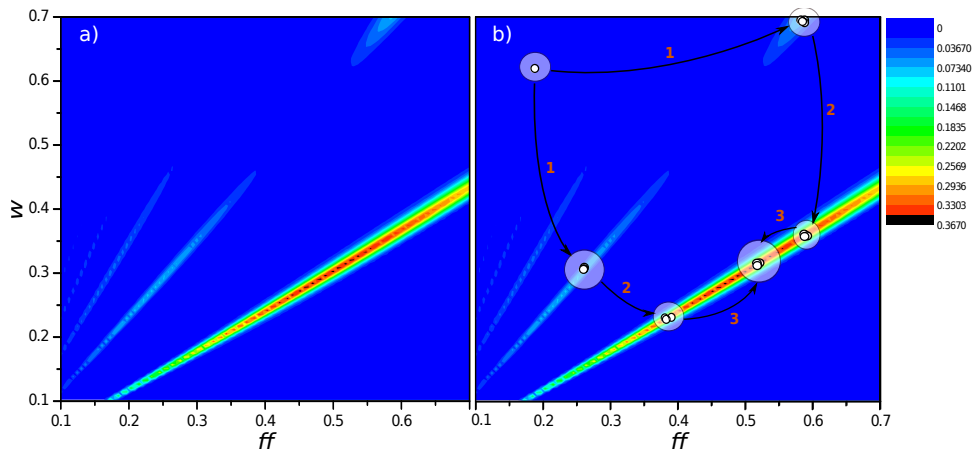


Figure 2. (a) The coloured chart depicts the coupling efficiency at $\lambda=1550$ nm for the entire set of W and ff combinations. (b) The solution dataset calculated by the IHS algorithm explained in Section 3 in (a) is over-imposed by circled set of points surrounded by a white cloud, showing the solutions given by this ID method at each iteration. The ID process clearly converges to the maximum coupling parameter pairs with low number of iterations in this toy model case, as detailed in Section 4 .

search for optimum coupling becomes futile. To counterbalance this issue, we have recently proposed a more efficient inverse design approach for designing photonic components that facilitates the prospect of optimum topologies in a rather variety of fields. This time, the ID method uses an IHS [8] algorithm as a core engine.

The HS algorithm [9] is a meta-heuristic optimization algorithm inspired by the observation of musical improvisation process, in which the aim is to search for a perfect state of harmony. HS was proposed by Geem et al. in 2001 and thenceforth it has been widely applied to a variety of combinatorial optimization problems [10–12]. During the process of musical improvisation, suggesting a new melody is subject to three different circumstances, a musician can either play a tune exactly in the way he has memorized it or he can play something similar to a stored melody (eg. slightly adjusting the pitch), or compose new notes randomly. Based on these three options, Geem et al. made a new quantitative optimization process. The three components analogous to the ones of musical improvisation became: memory usage of harmonies (HMCR), pitch adjustment (PAR) determined by a pitch bandwidth bw_{range} and randomization (RSR) [13].

In the original HS algorithm proposed by Geem in [9], the PAR and bw parameters are fixed and do not evolve during the optimization process. Therefore, the election of appropriate values for these operators becomes critical and the algorithm demands a high number of iterations for locating the global optimum state. In reference [8], however, the PAR and bw parameters are cyclically

tuned in order to achieve a smoother search, in a manner analogous to what the Cauchy-Lorentz probability distribution does in a Fast Simulated Annealing (FSA) algorithm [14]. In other words, the bw parameter must be set to high values in initial iterations in order to increase the diversity of solutions, but in final generations it must be set to low values to enhance the intensification and to sacrifice the diversification, that is, to search locally instead of globally. Throughout this work, we set a PAR_{min} and PAR_{max} parameters to 0.4 and 0.9. Then the bandwidth of each iteration $bw(n)$ is given non-linearly as:

$$bw(n) = bw_{max} \exp(c.n), \quad (2)$$

and the coefficient c is recalculated in each iteration as

$$c(n) = \frac{\ln \frac{bw_{min}}{bw_{max}}}{N}. \quad (3)$$

In order to cover a large number of solutions and to expand the search space in which diversification has a significant relevance, we set the minimum bandwidth, BW_{min} , to 0.0001; and the maximum bandwidth, BW_{max} , to 1. The $RSR \in [0,1]$, sets the probability of picking the value for the new note randomly from the domain of the input variables. It performs a role similar to the uphill jump probability function in the Simulated Annealing algorithm, but in this case the alteration in the harmony set stored in the memory of harmonies (HM) is performed regardless of its fitness with probability RSR . In this work we set the RSR parameter to 0.1. The HM is comprised of 20 harmonies, with 22 notes dilling each harmony. In the general case, where the etching deep of the groves is fixed, the first 20 notes belong to the period of each trench, bounded between a value of 0.15 μm and 0.5 μm . The two additional parameters are the SMF separation distance and the fibre tilt angle, bounded between 4 and 7 μm , and 8 and 15 degrees, respectively.

4 Speeding up: An heuristic engine for non-assisted exploration

It seems of practical relevance to check whether an ID process like the one described in [15] and using the IHS method of 3, gets to improved grating couplers or, conversely, if conventional periodic grating couplers fare better. In Figure 2.b the ID method results are over-imposed to the exhaustive lookup-map computed in Section 2. Noticeably, when using the ID methodology to this problem, the solution is quickly achieved taking into account only those combinations of parameters that yield to promising results. The ID method, boosted by IHS jumps quickly from average fitness solutions to local optima points and subsequently splits the search through local optima points to global optimum in just 3 iterations. The whole process takes only few minutes to converge to the solution remarked by white markers. Hence, even in this simplified model, introducing

the ID method drastically reduces the computation time and prevents the calculation of non-profitable solutions by determining the combination of parameters that enhances light overlapping between guide and fibre.

Some other optimization techniques could deal with this issues as well but either are based on gradient methods and tend to stack at local maxima or they provide lattices that are often not practical with current fabrication tolerances. Examples include exotic shaped designs that can barely be turned into operative designs using most advanced experimental prototyping techniques.

Due to this fact, it is convenient to constraint the optimization of theoretical designs to some parameters that render to a topology comprised by naive elements, that are closer to current fabrication facilities. In spite of this, there is no certainty of achieving a resulting device that operates as good as theoretical designs predictions. This is due to the fact that devising process always introduce some random errors that are independent of the design. In nanophotonics these errors can not be neglected as they may lead to produce totally different structures. In this regards, some authors have proposed to give design these devices by imposing in their designs the worst case analysis [16, 17]. The worst case analysis is a widely used approach in nowadays industry, but is still highly ineffective. On the one hand, it is not always easy to determine which of the configuration parameters yields to the worst case and in the other hand, a high restrictive proceeding forces to disregard many potentially good solutions.

5 Periodicity and aperiodicity, a comparison

The key features of an effective light coupling system are compactness, low insertion loss, large alignment tolerance, and broadband operation [2]. In a first attempt we took a 20 periods length grating profile with the parameters specified in Section 2, except that this time we led the ID algorithm decide the horizontal position of the SMF fibre, its tilt angle as well as the grating period, Λ . With this regards, we run the simulation and the grating was optimized for enhancing the coupling of light from the integrated waveguide to the SMF fibre. The final simulation set-up was found to be conformed by $\Lambda = 640 \text{ nm}$, with a fibre displaced $5.23 \text{ }\mu\text{m}$ from the grating edge and tilted 15° . By means of these values a maximum theoretical coupling efficiency of 66% is achieved with an estimated 1 dB bandwidth of 40 nm . According to the principle of interference, the Bragg conditions is fulfilled when

$$k_{in} \sin \Theta + m \frac{2\pi}{\Lambda} = \beta, \quad (4)$$

where $k_{in} = 2\pi/\lambda$ and $\beta = (2\pi/\lambda) n_{eff}$, being n_{eff} the effective refractive index of the structure. All in all, according to Equation 4 the grating period should be, for this particular case (for diffraction order $m = +1$, an angle of 15° and n_{eff} around 2.8):

$$\Lambda = \frac{\lambda}{n_{eff} - \sin \Theta}. \quad (5)$$

Equation 5 states that the optimum Λ for a λ of $1.55 \mu\text{m}$ should be 610 nm . This result is very close to the solution given by the ID method (640 nm). In fact, it should be pointed out that the Bragg condition is only exact for infinite structures, thus for finite structures, as long as in finite gratings there is not exactly one discrete wave-vector for which diffraction occurs, but for a range of wave-vectors. However, in periodic gratings the tuning of the wave vectors is limited by the period of the grating. The decay of the coupling performance for this structure is shown in Figure 3.a. The performance of the periodic grating converges when 20 grooves are etched in the silicon layer and the removal of grooves presents a polynomial decay of the coupling efficiency (see Figure 3.a). However, as one disposes of just 4 periods, the peak coupling efficiency starts to deviate from the target λ , as it is shown in Figure 3.b. This deviation amounts to 8 nm when only 10 periods are considered in the periodic grating.

Although the etching nonuniformity is usually detrimental for most applications, it can offer more freedom to realize a nonuniform grating coupler. However, designing such non periodic clusters entails dealing with several correlated parameters at the same time and cannot be designed using current analytic methods, or by tuning a small number of parameters by hand [19]. Nonetheless the ID method provides a prospect way for dealing with N -parameter look-up issues. In Figure 4.c a non-uniform grating coupler scheme is represented. In this particular case, every groove is detuned at the same time, constrained to fabrication limitations. The efficiency of the final corrugated waveguide yields to slightly better coupling results when compared to the former periodic case, depicted in Figure 4.b.

The solution obtained with the IHS algorithm provides a peak coupling efficiency of 69% with a 1 dB bandwidth close to 38 nm . Noticeably the grating structure depicted in Figure 4.c shows a smooth profile that ensures a good stability when the grating is shorten (see Figure 3.a.). In this case, the efficiency of the coupling almost corresponds to the periodic case. On the other hand, this grating profile enhances the coupling of light close to the $1.55 \mu\text{m}$ with a maximum deviation of 3 nm .

To further increase the efficiency of periodic gratings we should include the etching deep of the periodic grooves into the design process. However, according to Equation 5, these kind of gratings should be those with shallow deep etched profiles. With this regards, we headed on a different approach, i.e. we constrained the etching deep and the duty cycle of a non-uniform grating and we utilized the ID method for achieving a grating coupler that further enhances the light overlapping preventing full etching of the silicon layer or narrow grooves. The resulting grating profile is schematically shown in Figure 4.d. The simulated coupling spectrum for the TE polarization is shown in Figure 4.a for comparison. One can see that a maximum coupling efficiency of 78% is achieved at $1.55 \mu\text{m}$ and the 1 dB bandwidth is about 40 nm . The coupling efficiency is much larger than that for a standard uniform grating coupler and the wideband makes it very promising for C-band applications.

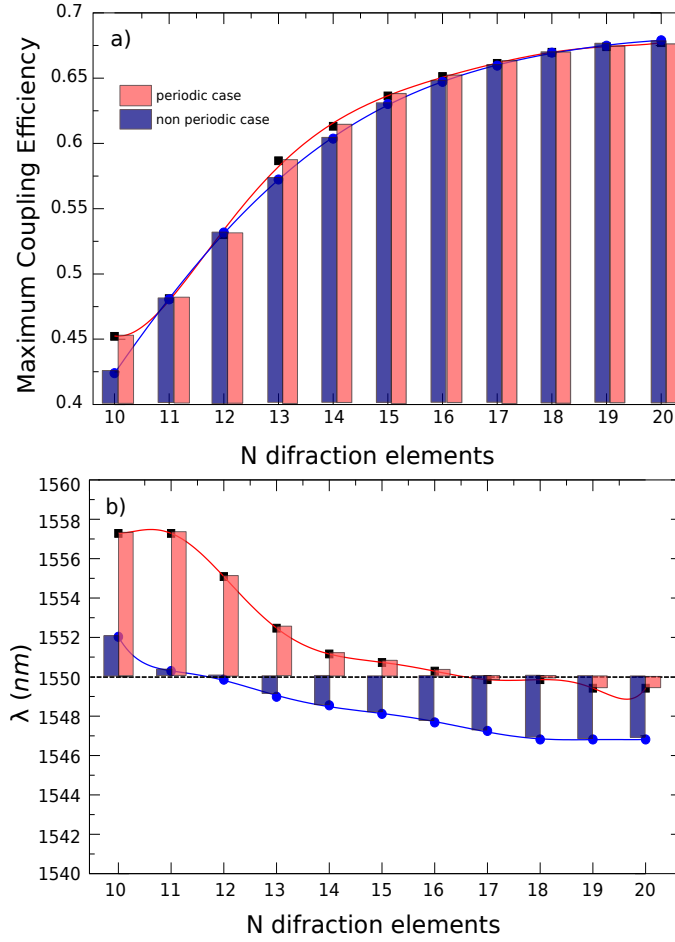


Figure 3. (a) Maximum coupling efficiency with regards to the number of grooves in the periodic and non-periodic gratings, sketched in red and blue respectively and (b) deviation of the peak coupling efficiency in each case.

6 Concluding Remarks

In this manuscript we demonstrate the great usefulness of using an inverse design approach to the process of exploring new grating coupler designs. By means of this method the designer can handle more parameters even when there is no theoretical background leading to any hints in the process of designing better couplers. We found that this methods are easily applicable to grating coupler design problems since they do not require great detailed knowledge of the structure of the problem and they can rely on the solver of the system as a blackbox. By this insight we found that the coupling efficiency of non-uniform grating couplers can outmatch custom periodic designs. Moreover, the structures proposed

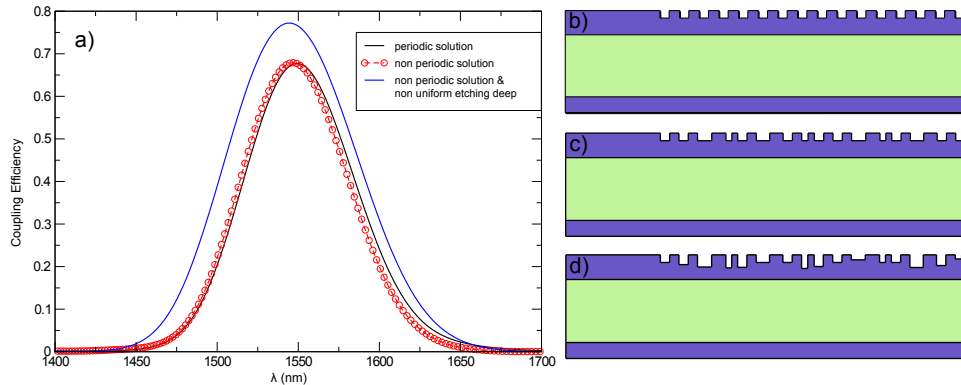


Figure 4. (a) Simulations results for coupling efficiency spectrum for each case of study. (b)-(d) The schematic representation of the optimized periodic grating, the aperiodic grating and the non-uniform grating made by also tuning the etch depth, respectively. The dimensions of the grooves have been exaggerated for clarity purposes.

in this work are fully compatible with conventional manufacturing processes as they prevent the formation of exotic geometries or shallow edges. The length of the non-uniform gratings is slightly shorter than that of canonical gratings. Besides, if these gratings are shortened, then they still hold for a reliable coupling ratio with a minimal deviation in the C-band.

References

1. J. V. Galan, *Addressing Fiber-to-Chip Coupling Issues in Silicon Photonics*, PhD Thesis, Universidad Politecnica de Valencia, (2010).
2. F. V. Laere, W. Bogaerts, D. Taillaert, P. Dumon, D. V. Thourhout, R. Baets *Grating Couplers for Coupling between Optical Fibers and Nanophotonic Waveguides*, *J. Lightwave Tech.*, 25, 151–156, (2007).
3. T. Shoji, T. Tsuchizawa, T. Wanatabe, K. Tamada, H. Morita, *Low loss mode size converter from 0.3 μm square Si wire waveguides to singlemode fibers*, *Electron. Lett.*, 38, 1669–1670, (2002).
4. D. Taillaert, F. V. Laere, M. Ayre, W. Bogaerts, D. Van Thourhout, P. Bienstman, R. Baets, *Japanese J. of Appl. Phys.*, 45, 6071–6077, (2006).
5. Y. Wang, X. Wang, J. Flueckiger, H. Yun, W. Shi, R. Bojko, N. A. F. Jaeger, L. Chrostowski, *Focusing sub-wavelength grating couplers with low back reflections for rapid prototyping of silicon photonic circuits*, *Opt. Express*, 22, 20652–20662, (2014).
6. R. Topley, L. O’Faolain, D. J. Thomson, F. Y. Gardes, G. Z. Mashanovich, G. T. Reed, *Planar surface implanted diffractive grating couplers in SOI*, *Opt. Express*, 22, 1077–1084, (2014).
7. D. Taillaert, *Grating couplers as Interface between Optical Fibres and Nanophotonic Waveguides*, PhD thesis, Universiteit Gent, (2005).
8. M. Mahdavi, M. Fesanghary, E. Damangir, *An improved harmony search algorithm for solving optimization problems*, *Applied Mathematics and Computation*, 188, 1567–1579, (2007).

9. Z. W. Geem, J. H. Kim, G. V. Loganathan, *A New Heuristic Optimization Algorithm: Harmony Search*, *Simulation*, 76, 60–68, (2001).
10. R. Forsati, A. T. Haghghat, M. Mahdavi, *Harmony search based algorithms for bandwidth-delay-constrained least-cost multicast routing*, *Computer Communications*, 31, 2505–2519, (2008).
11. Z. W. Geem, *Harmony Search in Water Pump Switching Problem*, *Advances in Natural Computation*, 3612, 751–760, (2005).
12. R. Zhang, L. Hanzo, *Iterative Multi-user Detection and Channel Decoding for DS-CDMA Using Harmony Search*, *IEEE Signal Processing Letters*, 16, 917–920, (2009).
13. I. Landa-Torres, S. Salcedo-Sanz, J. Del Ser, J.A. Portilla-Figueras, *Antenas*, *Expert Systems with Applications*, 39, 5262–5270, (2012).
14. H. Szu, R. Hartley, *Fast simulated annealing*, *Phys. Lett. A*, 122, 157–162, (1987).
15. I. Andonegui, I. Calvo, A. J. Garcia-Adeva, *Inverse design and topology optimization of novel photonic crystal broadband passive devices for photonic integrated circuits*, *Appl. Phys. A*, DOI:10.1007/s00339-013-8032-5, (2013).
16. O. Sigmund, *Manufacturing tolerant topology optimization*, DOI:10.1007/s10409-009-0240-z, (2009).
17. B. Momeni and A. Adibi, *Optimization of photonic crystal demultiplexers based on the superprism effect*, *Appl. Phys. B*, 77, 555–560, (2003).
18. I. Andonegui and A. J. Garcia-Adeva, to be publish.
19. A. Y. Piggott, J. Lu, T. M. Babinec, K. G. Lagoudakis, J. Petykiewicz, J. Vuckovic, *Inverse design and implementation of a wavelength demultiplexing grating coupler*, *Sci. Rep.*, 4, (2014).